Osteochondral Defect Repair of Large Weight-Bearing Surfaces in a Porcine Model

Brendan D. Stoeckl[1,2]
Kendall M. Masada[1,2]
Axel C. Moore[3,4]
Natalie L. Fogarty[1,2]
Elisabeth A. Lemmon[1,2]
Bijan Dehghani[1,2]
Lorielle G. Laforest[1,2]
James L. Carey[1,2]
Robert L. Mauck[1,2]
Molly M. Stevens3
David R. Steinberg[1,2]

[1]University of Pennsylvania, Philadelphia, PA, USA

[2]CMC VA Medical Center, Philadelphia, PA, USA

[3]Imperial College London, London UK.

[4]Carnegie Mellon University, Pittsburgh, PA, USA.

Introduction

Knee osteoarthritis represents an enormous clinical burden, but treatment for end-stage disease is limited to total knee replacement.[1] While often effective at limiting pain and restoring function, these metal and plastic devices begin to wear immediately upon implantation, and many eventually require costly and invasive revision surgeries.[2] Given this, earlier intervention through biologic cartilage reconstruction may be an ideal solution. Indeed, several interventions exist for early-stage cartilage damage, including osteochondral autografting or allografting in which an osteochondral unit from a non-weightbearing portion of the knee (or from a donor) is implanted into a defect site.[3] However, as with all biologic repair solutions, this procedure is only indicated in near-ideal surgical conditions, excluding the vast majority of patients with cartilage damage.[4] Thus, there exists a need for a large animal model which realistically assesses osteochondral repair in a clinically relevant disease setting, not only to improve strategies for expanding indications for existing technology, but also as a testbed for evaluating emerging therapeutics. In this study, we developed a large animal model (Yucatan minipig) of osteochondral defect repair on the weightbearing surface of the medial femoral condyle and evaluated the outcomes from clinical repair and a novel implantable scaffold.

Methods

Surgery was performed unilaterally in skeletally mature Yucatan minipigs. A medial parapatellar arthrotomy was followed by patellar subluxation and hyperflexion of the stifle to allow for visualization of the medial femoral condyle. Next, a 6mm diameter x 10mm depth defect was created using a standard Arthrex OATS® kit. A second defect, 7mm diameter x 10mm depth was created, and the resulting osteochondral plug was press-fit into the first defect. The empty 7mm defect served as a negative empty control. Each defect was made on the weight-bearing midline of the medial femoral condyle, and their relative positions proximal or distal were alternated between subjects. Animals were sacrificed 5 weeks after surgery, and joints were assessed grossly with India Ink staining. Next, medial femoral condyles were isolated, potted, and indented with a 2mm diameter spherical indenter in the center of, and 5mm adjacent to, each defect. Fifteen-minute duration creep tests at a 0.1N load were fitted to a Hertzian biphasic creep model,[5] and values for compressive modulus, tensile modulus, and permeability were determined. Contralateral medial condyles were tested as a positive control. Next, osteochondral tissues were scanned via microCT before and after immersion in Lugol's solution to enhance the radiopacity of the cartilage. Finally, osteochondral units

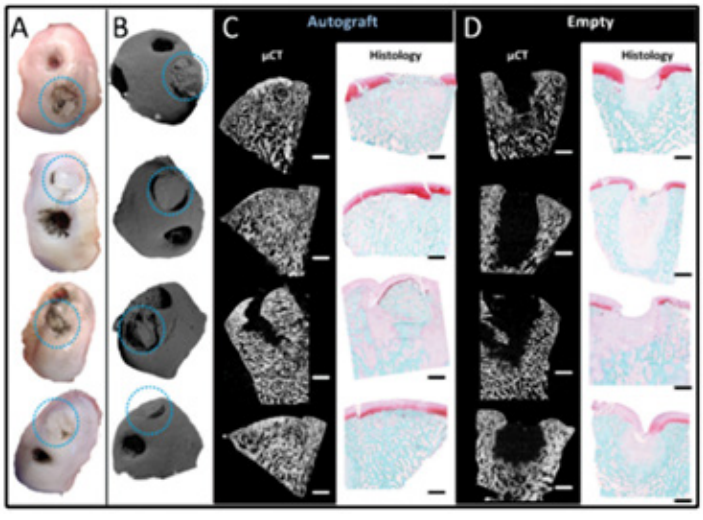

Figure 1. (A) Gross India ink-stained images of medial femoral condyles showing autograft repair (blue circles) and empty defects after 5 weeks in vivo. **(B)** 3D μCT reconstructions of condyles from 1A. **(C)** Sagittal 2D slices from μCT and Safranin-O/fast green stained sections of autograft repair and **(D)** empty defects. Scale = 1mm.

were decalcified, paraffin processed, embedded, sectioned, and stained with Safranin O/Fast Green to visualize matrix content. In follow-on studies, this same model was used in a second set of animals to test the efficacy of a synthetic, acellular, osteochondral construct. The osteochondral implant (Figure 3A) was composed of two components: (1) a poroelastic cartilage mimic and (2) an osseointegrating bone substitute. The poroelastic mimic, FiHy™, is described in.[6] The bone substitute was formed by direct printing of poly(e-caprolactone) onto FiHy™. This direct printing approach enabled a strong interfacial bond between the cartilage mimic and bone substitute and eliminated the need for adhesives for mechanical fixation. Eight mm diameter constructs were fabricated and press-fit into the 7mm osteochondral defect created while forming the autograft plug as described above. Scaffold-filled defects were analyzed as above at the 5-week time point. All quantitative data were compared with one-way ANOVA followed by Tukey's post hoc tests, with significance set at $p < 0.05$.

Results

Based on gross images (Figure 1A) and 3D reconstructions of μCT (Figure 1B), autograft implants remained in the defect at the 5-week timepoint and maintained congruence with the cartilage surface of the condyle. 2D μCT slices showed excellent implant integration with the surrounding bone in 3/4 specimens analyzed, while histology showed variable losses in proteoglycan content in the cartilage (Figure 1C). Empty defects showed persistent deficits in both bone and cartilage (Figure 1D). Both empty defect repair tissue and autograft cartilage were mechanically weaker than contralateral cartilage (Figure 2). However, autograft cartilage was significantly stronger than empty defect repair tissue and was not different from cartilage adjacent to the defect (Figure 2). Synthetic osteochondral constructs (Figure 3A) remained fully seated in the defect as evidenced grossly (Figure 3B) and via μCT (Figure 3C-E), with some evidence of bony integration (Figure 3D) at this early time point.

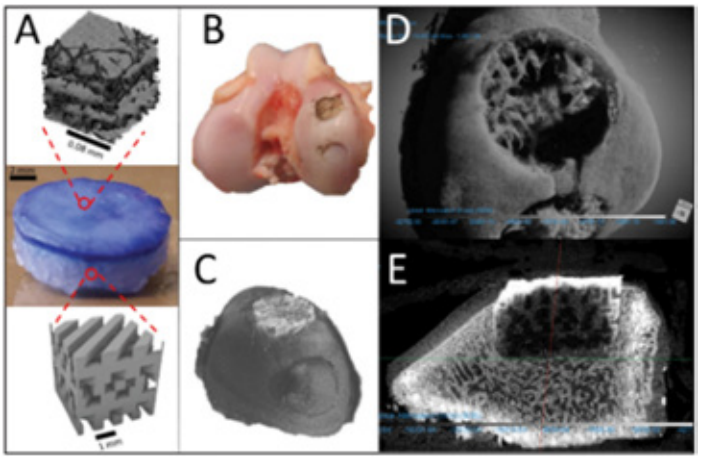

Figure 3. (A) Osteochondral implant consisting of a poroelasic cartilage mimic and a 3D printed PCL osseointegrating component. **(B)** Synthetic implant (top) and autograft (bottom) with India ink staining in the pig medial femoral condyle after 5 weeks in vivo. **(C)** 3D rendering of contrast-enhanced μCT. **(D)** Evidence of mineralized tissue within the implant. **(E)** 2D slice of contrast enhanced μCT showing implant remaining in and fully filling the defect.

Discussion

In this study, we developed a porcine model of large, osteochondral repair on the weightbearing surface of the medial femoral condyle. Most interestingly, it appears that even in the near ideal surgical conditions (healthy knee, fresh autograft implant) used here, implant tissue was mechanically weaker than native after only 5 weeks in vivo. This indicates that there may be room for adjuvant therapies to enhance the repair of large defects, even when fresh autograft tissue is available. This work also demonstrated the potential efficacy of an acellular biphasic poroelastic construct for osteochondral repair. Ongoing work includes quantitative analysis of μCT and scoring of histology, extending to longer time points and evaluating other engineered materials. Future work may further increase the usefulness of this model by inducing a degenerative phenotype in the knee [7] and assessing osteochondral repair in such a clinically typical, but rarely studied environment.

Significance

This study develops a clinically relevant model for assessing osteochondral repair in large weight-bearing defects.

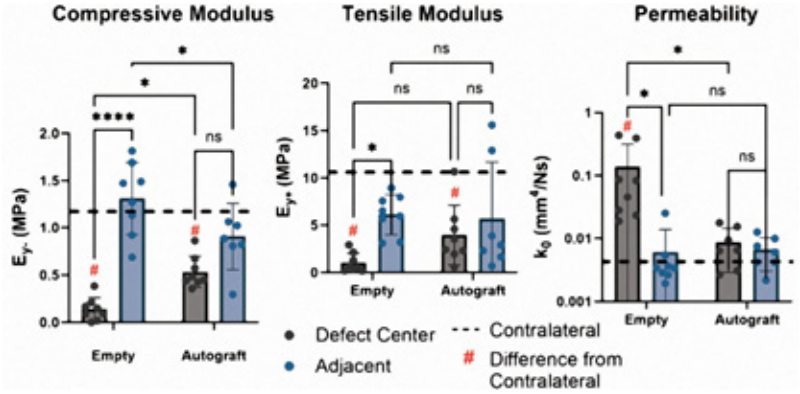

Figure 2. Results of creep indentation tests fitted to a hertzian biphasic model. * = p<.05; **** = p<.0001.

References

1. Devitt B, Bell S, Webster K *et al.* Surgical treatments of cartilage defects of the knee: Systematic review of randomised controlled trials. *Knee*. 2017 Jun;24(3):508-517

2. Bayliss L, Culliford D, Monk A *et al.* The effect of patient age at intervention on risk of implant revision after total replacement of the hip or knee: a population-based cohort study. *Lancet*. 2017 Apr 8;389(10077):1424-1430

3. Hangody L, Karpati G, Szerb I, *et al.* Arthroscopic autogenous osteochondral mosaicplasty for the treatment of femoral condylar articular defects. A preliminary report. *Knee Surgery*. 1997;5(4):262-7

4. Martin A, Patel J, Zlotnick H, *et al.* Emerging therapies for cartilage regeneration in currently excluded 'red knee' populations. *NPJ Regen Med*. 2019 May 30:4:12.

5. Moore A, DeLucca J, Elliott D, *et al.* Quantifying Cartilage Contact Modulus, Tension Modulus, and Permeability With Hertzian Biphasic Creep. *J Tribol*. 2016 Oct;138(4):0414051-414057

6. Moore A, Hennessy M, Nogueira L, *et al.* Fiber reinforced hydrated networks recapitulate the poroelastic mechanics of articular cartilage. *Acta Biomaterialia*. 2023 Sep 1:167:69-82

7. Stoeckl B, Meadows K, Bonnevie E *et al.* Surgical Reattachment of the Anterior Horn Slows OA Progression in a Large Animal Injury Model. *ORS*. 2022.